# STEADY-STATE ONE-DIMENSIONAL BREAKDOWN OF THERMOPLASTICS UNDER HEAVY FLUXES OF RADIANT ENERGY

N. P. Novikov, V. P. Perminov, and A. A. Kholodilov

UDC 536.37:678.073

It is shown that part of the breakdown in specimens of polystyrene (PS) and polymethylmetacrylate (PMMA) is nonthermal. The thermal breakdown parameters as well as characteristics of the vapor-condensate zone and the linear velocity of the breakdown front have been measured. The results of the experiment are interpreted theoretically.

The breakdown of thermoplastics, namely polymethylmetacrylate (PMMA) and polystyrene (PS) under a heavy flux of radiant energy is of considerable scientific as well as practical interest. An experiment was performed under conditions ensuring a one-dimensional process flow, which made it possible to simplify the theoretical analysis. New results were obtained, indicating the three-dimensional character of such a breakdown, and an interpretation will be proposed here. The procedure followed here allows the problem to be greatly simplified and it offers some definite advantages: a) the breakdown zone is extended and, therefore, its structure can be thoroughly examined; b) the radiant flux density is measured during the tests, which makes it possible to establish the relation between polymer surface temperature, radiant flux, and linear velocity of the breakdown front. The thermal decomposition of polymers was studied by other methods in [1-5]. Thermal breakdown under a jet of high-temperature plasma was studied in [1, 2]. It has been shown there that most of the breakdown is due to interaction between the plasma and the material. Under heavy radiant fluxes ($\sim$1 kW/cm$^2$) the breakdown (wear) rate of materials such as Teflon and polyethylene is determined by the rate at which the carbon film on the surface evaporates, while in the case of materials like PS and PMMA the specific cause is bulk pyrolysis due to the energy of thermal fluctuations accompanied by a generation of gaseous products almost across the entire specimen thickness and the exhaust of gases through the layer of softened material. The method of a hot plate pressed against a specimen was used in [3], in [4] breakdown was effected by means of a propane burner with a plane flame front. It has been established in [5] that the breakdown front advances slower when PMMA breaks down under a $CO_2$ laser and craters are formed in bulky specimens. In our study this phenomenon is explained as follows: in front of the breaking down surface there form minute particles which absorb radiation and the radiant thermal flux is dissipated on widening the crater. In the experiments which will be described here the heavy flux of radiant energy was generated by a gaseous $CO_2$ laser on the wavelength $\lambda = 10.6\ \mu$ [6]. In this range of wavelengths ($\lambda = 10.6\ \mu$) the materials under study, namely PMMA and PS, are almost opaque and all the laser radiation is completely absorbed by specimens. In all tests the laser radiation was carefully checked and recorded on a model S-1-19 oscillograph through a model ÉPP-09 potentiometer with a photoresistor.

The tests were performed by the following procedure. The laser beam 6 mm in diameter was transmitted through a mechanical shutter and the inlet window in a vacuum chamber (residual pressure 0.01 mm Hg), impinging there on a cylindrical specimen approximately 4 mm in diameter. In order to eliminate any lateral heating, the specimens were encapsulated. In front of a specimen, at precisely selected distances and perpendicularly or parallel to the laser beam (but contained within its boundaries) were placed NaCl plates with a high surface polish on which the products of decomposition deposited within a very short time. These deposits were then examined under a model MB1-3 microscope or replicas of the plates were

Institute of Problems in Mechanics, Academy of Sciences of the USSR, Moscow. Translated from Inzhenerno-Fizicheskii Zhurnal, Vol. 23, No. 2, pp. 257-266, August, 1972. Original article submitted July 9, 1971.

examined under a model Elmi D-2 electron microscope. The described procedure made it possible not only to study the specifics of the decomposition products but also to determine their size, number, and mass distributions at various distances from the surface. The chemical makeup of the decomposition products was determined from infrared spectra on a model IKS-14A spectrophotometer with an NaCl prism. These spectra were compared with those of the original materials and their monomers. Photographing the breakdown process in a specimen from the side at definite time intervals made it possible to determine the breakdown rate (within a 5% accuracy) and other characteristics. By comparing the photographs of a breaking down specimen at various instants of time, it was possible to assess the stability of the process.

The temperature of specimens during tests was measured with carefully calibrated thermocouples of two types: copper–constantan ~30 $\mu$ round wires and tungsten–rhenium 10 $\mu$ thick ribbons. The signals from the thermocouples were fed through a dc amplifier and then recorded on a model N-105 loop oscillograph. Four to six thermocouples were precisely spaced axially along a specimen. From these measurements one could not only determine the temperature distribution in a breaking down specimen but also, by comparing the readings of the various thermocouples in one specimen, it was possible to assess the stability of the process. The accuracy of temperature measurements was better than 3%. The process stability was checked on the basis of photographs showing the specimen breakdown at definite time intervals and of the temperature distributions recorded at various points inside the specimen. The photographs have established that the breakdown character remains the same throughout the time of laser action. The breakdown of a specimen in these tests approached the analogous process in [4, 5] and was, regardless of the material, characterized by minute bubbles near the breakdown surface as well as by a "heat wave" [5]. From the temperature distribution near the breakdown front in a PMMA specimen (Fig. 1) it appears that the temperature curves are exactly the same at various points in the specimen. This is also an indication that the thermal breakdown processes are stable. Thus, the breakdown of thermoplastics in these tests was one-dimensional and steady.

The curves in Fig. 1 indicate that the temperature varies exponentially along the specimen axis.

The tests have shown that, as the power of laser radiation is increased, the temperature at the breakdown front rises but does not exceed 500°C. Taking into account that the state of a breaking down specimen material is a function of the temperature, the region of thermoplastic breakdown can be subdivided into four spatial zones, each with a completely defined temperature distribution (Fig. 2). In zone I the polymer is solid and the temperature is distributed exponentially according to Michelson's law, $T_c$ denoting the temperature of softened material. At this point there occurs a jump change in the heat capacity. In zone II the polymer is superelastic. In zone III the quasifluid polymer begins to undergo pyrolysis (thermal breakdown) with rising temperature. In zone IV the polymer consists of tiny droplets formed by the fragmentation of the quasifluid polymer. The veil of droplets consists of semifused polymer particles which are further converted by the radiation and gradually "burnt out." In zone V the decomposition products are gaseous.

A comparison of the photographs of the breakdown process with the temperature curves indicates softening of the material at 150°C, as has also been found in [5]. The softening temperature is the practical threshold of zone II and coincides with the "heat wave" front [5]. From this comparison one can also determine the instant at which a thermocouple emerges at the breakdown surface of the specimen, i.e., determine the surface temperature (this temperature depends on the incident radiation power and at W = 10 cal/cm$^2$ · sec, for example, is T = 370°C for PS and T = 430°C for PMMA). This temperature is the practical threshold of zone III. The beginning of this zone is defined by the bend of the temperature curve ($T_b$ in Fig. 2). The tests have shown that a thermocouple reflects almost all the incident radiation and does not heat up in a laser beam, making it feasible to measure the temperatures in zones IV and V. After a thermocouple had become exposed to the laser beam in front of the breakdown surface (zones IV and V), according to the trend of temperature curve 5 (Fig. 1), the temperature remains almost constant but fluctuates in front of the specimen due to the peculiar structure of the flux (which will be discussed later). Zones IV and V can be discerned only on the basis of an analysis of decomposition products within these two zones. Thus, from the test results one can establish the various zones of polymer breakdown characterized by their peculiar temperature distributions.

In Fig. 3 is shown the length of breaking down PMMA and PS specimens as a function of exposure time to laser radiation. The exposure time is laid off along the axis of abscissas from some instant already after the process has begun, i.e., the process here is considered steady. On the basis of these graphs, one can determine the linear velocity of the polymer breakdown front, this velocity remaining almost constant during exposure to radiation and increasing with higher radiation power. The scatter of test points is

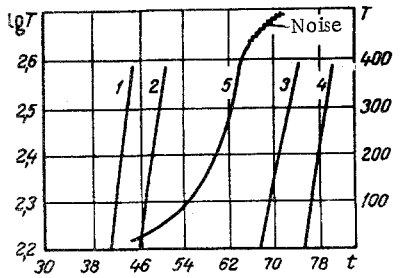


Fig. 1

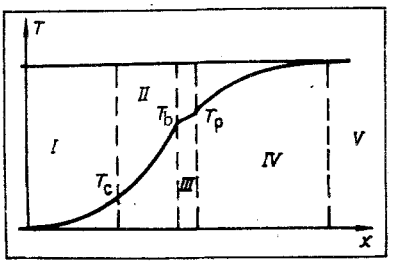


Fig. 2

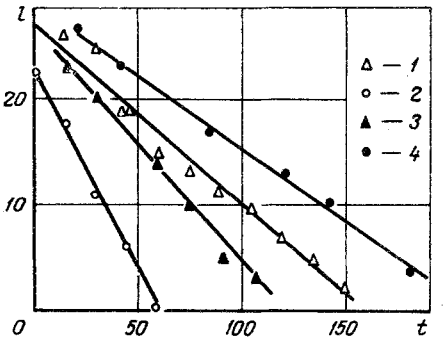


Fig. 3

Fig. 1. The logarithm of temperature (°C) as a function of time (sec), based on thermocouple readings at various depths below the original specimen surface (left-hand axis of ordinates): 1) 7 mm; 2) 8; 3) 12; 4) 13; the specimen temperature as a function of time, based on one thermocouple (right-hand axis of ordinates): 5) 10 mm.

Fig. 2. Zones in a breaking down specimen.

Fig. 3. Length of PS specimens (1, 2) and PMMA specimens (3, 4) as a function of exposure time: 1, 3) $W = 10$ cal/cm$^2$ · sec; 2, 4) 6.

due to the measurement error as well as possibly due to the breakdown specifics: the periodic formation of an absorption zone in front of the breakdown surface.

The tests have shown that the stream flowing off the breakdown surface contains a mixture of gaseous products, condensate droplets, and solid pieces. Photographs of deposits are shown in Fig. 4. In Fig. 4a are shown decomposition products, predominantly liquid: droplets seem to spread over the surface. The shape of solid pieces does not change and there appears no such spreading (Fig. 4b), although the peculiar "tail" (marked with an arrow) indicates liquid polymer on their surfaces (solid pieces covered with a liquid film). Probably, solid particles have come out of the specimen and melted in the incident radiant flux in front. Gaseous decomposition products, while striking the surface, form droplets of condensate uniformly spread over the entire surface. The "droplet" density increases with the distance from the specimen surface,* which is entirely natural (as a result of evaporation of solid and liquid formations). The predominance of one or another component (of the three) near the breakdown surface is in a direct relation to the power of the acting laser flux (only vapor exists at above 12 cal/cm$^2$ · sec, droplets of liquid predominate within the 8-10 cal/cm$^2$ · sec range, and the solid phase predominates within 6-8 cal/cm$^2$ · sec.

The vapor-condensate structure of the stream in front of the breakdown surface determines the characteristic noise signal from the thermocouples emerging in zone IV, as a result of successive deposition of large single droplets or pieces on the thermocouples. It is noteworthy that a comparison of the temperature trend in [4] with the temperature distribution in our tests provides clues to the nature of the noise signal from thermocouples which is generated as the breakdown front moves. An analysis of infrared absorption shows that in all cases at all given levels of radiation density the spectra of decomposition products correspond exactly to the spectra of original materials, although differences between the molecular weight of the original material and that of the deposited material are possible as a result of thermal breakdown. Such a difference has not been established by spectral analysis, and the molecular weights were not measured. For this reason, we have indicated earlier that the material in the vapor-condensate zone is a polymer in a mixture of states.† Thus, in front of the breakdown surface there forms a vapor-condensate zone containing the various phases of the polymer material, with either one phase predominant depending on the power of active radiation.

In Figs. 5 and 6 are shown graphically the number and the diameter of polymer particles in the stream, as functions of the distance from the breakdown surface. The number and the diameter of particles both decrease with increasing distance, which has to do with the transition of polymer into the gaseous phase, i.e., with its particular "burnt out." The diameter d as well as the number of particles n are

* The measurements were made at distances not less than 2 mm from the specimen surface.

† An appreciable absorption of laser radiation by the material in front of the breakdown surface was indicated in [5], and is now explained.

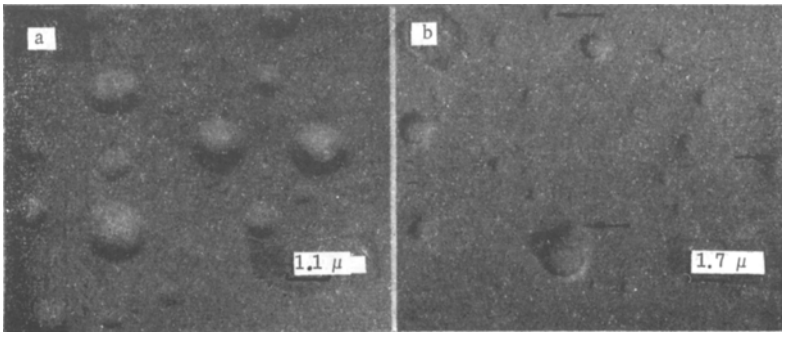


Fig. 4. Particles of vapor-condensate zone: a) liquid phase predominant; b) solid phase predominant.

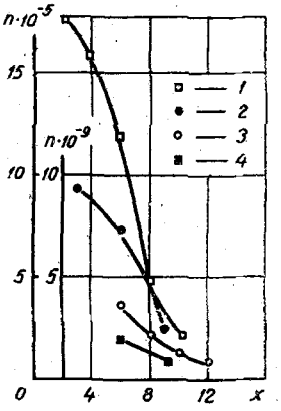


Fig. 5

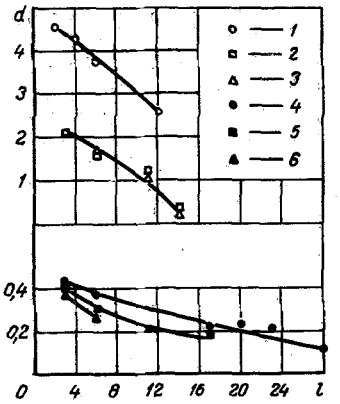


Fig. 6

Fig. 5. Concentration of particles. PS dimension is number of particles $n \cdot 10^{-5}$ $cm^{-2}$ (ordinate axis to the left): 1) W = 12 cal/$cm^2$ · sec; 2) 10. PMMA dimension is number of particles $n \cdot 10^{-9}$ $cm^{-2}$ (ordinate axis to the right): 3) W = 12 cal/$cm^2$ · sec; 4) 10.

Fig. 6. Diameter of particles d ($\mu$). PS (blank points): 1) W = 6 cal/$cm^2$ · sec; 2) 10; 3) 12. PMMA (black points): 4) W = 6 cal/$cm^2$ · sec; 5) 10; 6) 12.

nonlinear functions of the distance. The trend of these curves does not depend on the specimen material, although there are some specific data available which show various absolute values of d and n corresponding to the same distance. Since the veil of condensate (zone IV) near the breakdown surface absorbs and disperses the laser radiation, hence the flux density near the breakdown surface should naturally be lower than the incident flux density. For convenience, we have everywhere indicated only the incident radiation density. Thus, the tests show that the breakdown under a heavy thermal flux is not just a pyrolytic but quite a complex process.

The results of these experiments yield a simple explanation for the occurring phenomenon which is based on the heat balance within the breakdown process. The authors propose the following model of the process: a heavy radiant flux, after impinging on the specimen surface, is absorbed by the latter and causes its thermal breakdown. As a result, a vapor-condensate layer forms near the surface. This layer absorbs and disperses part of the incident radiation. Knowing the magnitude of the radiant flux which has passed through this vapor-condensate layer, one can determine the rate of specimen breakdown.

We will explain the causes of such a vapor-condensate layer formation in front of a specimen, which has, above all, to do with the structure of the tested polymers. PMMA and PS are polymers with a definite supramolecular structure and a rather high porosity [7]. Supramolecular formations of PMMA are defined by domains 1-10 $\mu$ in diameter with weaker intermolecular than intramolecular bonds and pores mainly at the boundaries. The basic formations in PS are globules joined into "zones" with well defined boundaries [7]. A thermal flux generates gas both at the surface and inside a specimen, which then fills the pores. As

TABLE 1. Specimen Fraction Breaking Down Nonthermally

| Material | W, cal/cm²·sec | ρ, g/cm³ | c, cal/g·deg | $l_0$, cal/g | $(T-T_0)$, °C | $V_b$, cm/sec | $\varepsilon = \frac{V_{bm}-V_{bc}}{V_{bm}}$ |
|---|---|---|---|---|---|---|---|
| PMMA | 10 | 1,2 | 0,4 | 380* | 415 | 0,019 | 0,2 |
| PS | 10 | 1,1 | 0,32 | 255 | 348 | 0,0394 | 0,37 |

*The value of $l_0$ is taken from [12].

a result, the polymer breaks down along the zone of domain boundaries and a vapor-condensate layer forms in front of the specimen. As W is increased, the surface temperature rises, a layer of melted polymer forms, and liquid droplets are ejected. By reducing the thermal flux density, it is possible to establish its level at which thermal breakdown only occurs on the surface. Thus, a specimen breaks down not only on the surface (thermal breakdown) but also throughout some layer.

We will now propose a method of roughly estimating the fraction of a polymer specimen which, though breaking down, is not destroyed. From the conventional equation of heat balance we can determine the breakdown rate $V_{bc}$ for a specimen:

$$V_{bc} = \frac{W}{\rho\left[l_0 + c\left(T_s - T_0\right)\right]}, \tag{1}$$

with $\rho$ denoting the polymer density; c denoting its specific heat; $T_S$ denoting the measured surface temperature; and $l_0$ denoting the total depolymerization energy. As has been shown earlier, however, breakdown occurs at the boundaries of supramolecular formations. Naturally, the measured velocity of the breakdown front ($V_{bm}$) is in this case higher than the calculated rate $V_{bc}$. A comparison between $V_{bm}$ and $V_{bc}$ will yield the specimen fraction $\varepsilon$ breaking down nonthermally. The results of these estimates are given in Table 1. It is evident here that this fraction is smaller in PMMA than in PS, which can be explained by the lower depth to which thermal flux penetrates into a PS specimen.

Indeed, since the radiation power at the surface of a breaking down specimen is lower than the incident power, because of attenuation in the vapor-condensate layer, hence it is necessary in (1) to add an appropriate correction to the value of W, which will widen the difference between $V_{bm}$ and $V_{bc}$ and thus increase the specimen fraction breaking down nonthermally. This correction will be determined subsequently.

Let us estimate the laser radiation in a vapor-condensate layer. We will consider the steady-state case. Such a layer consists of polymer particles whose diameter is $d \leq \lambda$ and, therefore, both absorption and dispersion must be taken into account. When a layer is optically thin, the transmitted light intensity (with absorption and dispersion accounted for) can be found as follows [8, 9]:

$$W(x) = W(\infty)\exp\left[-k_0 m(x)\right], \tag{2}$$

where m(x) denotes the total mass of particles in a column from x to $\infty$ and 1 cm² in cross section, while the constant $k_0$ represents the optical properties of the polymer material. Under steady process conditions, disregarding any heat conduction, the equation of heat balance for the layer can be written as follows:

$$W(x) = W(\infty)\exp\left[-k_0 m(x)\right] = \rho V_b\left[l_0 + c\left(T(x) - T_0\right)\right] + V l_0 \frac{dm}{dx}, \tag{3}$$

with W(∞) denoting the incident radiation flux, the x-coordinate measured from the breakdown surface into the layer; $l_0$ denoting the latent heat of monomer evaporation and the energy of thermal destruction of the polymer molecule; T(x) denoting the temperature at a given section; and V denoting the steady-state velocity of the particle stream. Function W can be found from the condition of equilibrium between an evaporating droplet and the radiation flux at a given section [10]:

$$W(x)\,Q_a = n_s l_0 \frac{kT(x)}{h} \cdot \frac{F^{+}}{F} \exp\left[-\frac{l_1}{kT(x)}\right], \tag{4}$$

where $Q_a$ is the absorptivity of a spherical droplet [8]. The maximum temperature $T_1$ in a vapor-condensate layer can be found from the condition

$$W(\infty)\,Q_a = n_s l_0 \frac{kT_1}{h} \cdot \frac{F^{+}}{F} \exp\left[-\frac{l_1}{kT_1}\right], \tag{5}$$

TABLE 2. Mass Distribution in Vapor-Condensate Zones

| Material | $W$, cal/cm$^2$/sec | $m_0$, g/cm$^2$ | $V_b$, cm/sec | $k_0 m_0$ | $W_0 \exp(-k_0 m_0)$ |
|---|---|---|---|---|---|
| PS | 6 | $1{,}43 \cdot 10^{-5}$ | 7,3 | $2{,}2 \cdot 10^{-3}$ | 6 |
| PMMA | 10 | $(0{,}8-1{,}6) \cdot 10^{-3}$ | 2 | $(1{,}2-2{,}5) \cdot 10^{-1}$ | (5–7,5) |

where $n_S$ denotes the surface density of monomer molecules in a droplet; k is the Boltzmann constant; h is the Planck constant; and $F^{\ddagger}$ is the statistical sum of activated complex material.

The total radiant flux on the material surface is determined from the full temperature profile in the vapor-condensate layer, but for integrating Eq. (3), we replace T(x) by $T_1$ with little effect on the mass distribution and, besides, because we are only interested in the total mass m(x) at a given section. We also assume that the entire mass of condensate is converted to a monomer at a sufficiently large distance, and then

$$W(\infty)=\rho V_b\left(l_0+c(T_1-T_0)\right). \tag{6}$$

Integrating Eq. (3) under condition (6) yields

$$\frac{e^{k_0 m(x)}-1}{e^{k_0 m_0}-1}=\exp\left(-\frac{k_0 W(\infty)}{V l_0}\,x\right). \tag{7}$$

In order to determine $m_0$, we use the boundary condition

$$\lambda\frac{dT}{dx}=W(\infty)e^{-k_0 m_0}. \tag{8}$$

Let the thermal conductivity be $\lambda$ = const, then

$$m_0=\frac{1}{k_0}\ln\frac{W(\infty)}{c\rho(T_s-T_0)V_b}. \tag{9}$$

Finally, we have

$$W(x)=\frac{W(\infty)}{1+\left(\dfrac{W(\infty)}{c\rho V_b(T_s-T_0)}-1\right)\exp\left(-\dfrac{k_0 W(\infty)}{l_0 V}\,x\right)} \tag{10}$$

and the mass distribution

$$\exp\left(m(x)k_0\right)=1+\left(\frac{W(\infty)}{c\rho V_b(T_s-T_0)}-1\right)\exp\left(-\frac{k_0 W(\infty)}{l_0 V}\,x\right). \tag{11}$$

Inserting (10) into (4), one can calculate T(x) and, inserting W(0) into (1), again determine $V_{bc}$ and compare it with the experimentally determined linear velocity of the breakdown front. An analysis of the relation m = f(x) shows that in the practically important case of rather large distances x and $m_0 k_0 < mk < 1$

$$m(x)=m_0\exp\left(-\frac{k_0 W(\infty)}{l_0 V}\,x\right). \tag{12}$$

As $x \to 0$, the exponential relation becomes logarithmic. In this way, within the framework of our model it is possible to almost completely solve the problem of mass and temperature distribution in a vapor-condensate layer when radiation from a gas laser acts on a thermoplastic material. This suggested mechanism implies that the process is not affected by the rate of chemical decomposition, the latter stabilizing at such a level as to ensure the necessary passage of material into the vapor-condensate zone.

We will estimate the value of $k_0$. According to [9], $k_0$ can be expressed as

$$k_0=\frac{36\pi n\varkappa}{\rho(m^2+2)^2}\cdot\frac{1}{\lambda};\quad \varkappa=\frac{\lambda\alpha}{4\pi},$$

so that $k_0 = 9n\alpha/\rho(n^2+2)^2$ when $m = n - i\varkappa$, $\lambda = 10.6\ \mu$, and $\rho = 1.2\ \mathrm{g/cm^3}$. Assuming n = 1.5 for both

polymers and $\alpha = 250$ cm$^{-1}$ for PMMA but $\alpha = 55$ cm$^{-1}$ for PS,* we have $k_0 = 156$ cm$^2$/g for PMMA and $k_0 = 34.4$ cm$^2$/g for PS.

With the aid of particle number and diameter distribution curves, we will determine the mass distribution in a vapor-condensate layer. Results of these calculations are given in Table 2, together with the values of incident laser radiation density $W(\infty)$ and laser radiation density reaching the specimen $W' = W(\infty) \exp(-k_0 m_0)$. The difference between $W(\infty)$ and $W'$ is most appreciable at heavy fluxes, especially in the case of PMMA, but in the case of PS the shielding effect of the vapor-condensate layer is weak. Thus, one notes that the vapor-condensate layer has an essential shielding effect, stronger in PMMA and weaker in PS.

With the true value of $W(x)$ reaching the surface, we again determine for PMMA the specimen fraction breaking down nonthermally: for $W(\infty) = 10$ cal/cm$^2 \cdot$ sec and $W' = 5.0$–$7.5$ cal/cm$^2 \cdot$ sec, $\varepsilon = 0.5$ (earlier we obtained $\varepsilon = 0.2$). For PS this fraction varies extremely little, inasmuch as $W'$ differs only slightly from $W(\infty)$ at the given power level.

In conclusion, we will make one more estimate. The thermal diffusivity $a^2$ can be determined from a measurement of the temperature distribution near the breakdown front in PMMA or PS. Under steady-state conditions and without chemical agents present, the temperature distribution in a specimen can be written as

$$T(x) = T(0) \exp\left(-\frac{V_n x}{a^2}\right). \tag{13}$$

Comparing this distribution with the one determined experimentally, one can determine $a^2$ if the linear velocity of the breakdown front $V_b$ is known. In this way, we have found $a^2_{PS} = 10^{-3}$ cm$^2$/sec and $a^2_{PMMA} = 2.6 \cdot 10^{-3}$ cm$^2$/sec. These values agree closely with published data [11], they thus provide a sound basis for checking the temperature and process stability measurements.

## LITERATURE CITED


1. Yu. A. Buevich and M. I. Yakushin, Prikl. Mekh. i Tekh. Fiz., No. 1 (1968).
2. Yu. A. Buevich, O. K. Egorov, and M. I. Yakushin, Prikl. Mekh. i Tekh. Fiz., No. 4 (1968).
3. R. F. Chaiken et al., J. Chem. Phys., 32, No. 1 (1960).
4. R. F. McAlevy et al., AIAAJ, 6, No. 6 (1968).
5. D. P. Krindach, N. P. Novikov, and Yu. I. Yudin, Mekh. Polimer., No. 2 (1968).
6. N. N. Sobolev, Usp. Fiz. Nauk, No. 3 (1967).
7. N. P. Novikov, A. A. Kholodilov, F. N. Chernyavskii, and V. A. Kargin, Dokl. Akad. Nauk SSSR, No. 6 (1968); No. 2 (1967); VMS, No. 2 (1970).
8. Van der Hulst, Dispersion of Light by Small Particles [Russian translation], IL, Moscow (1961).
9. K. S. Shifrin, Dispersion of Light in a Turbid Medium [in Russian], Izd. GTTL, Moscow (1951).
10. S. Glasston, K. I. Leider, and Ayring, Theory of Absolute Reaction Rates [Russian translation], IL, Moscow (1948).
11. E. P. Subbotina, in: Physical Constants and Parameters [in Russian], Izd. LGU, Leningrad (1967).
12. E. V. Tkachenko, V. B. Ulybin, and A. S. Shteinberg, Fiz. Gorel. Veshch., No. 1 (1969).


*The values of $\alpha_{PMMA}$ and $\alpha_{PS}$ have been determined experimentally.